Egypt. J. Chem. **Vol. 67,** No. 4 pp. 353 - 359 (2024)

Egyptian Journal of Chemistry

http://ejchem.journals.ekb.eg/

A Novel Treatment of Phenolic Wastewater Using Recyclable Rubbery Carrier for Heterogeneous Fenton's Process

S.M. Salem-Gaballah [a*], M.K. Fouad [b], F.I. Barakat [b], Aliaa Abdelfatah [b]

[a] *Faculty of Science, Cairo University, Giza, Egypt*

[b] *Faculty of Engineering, Cairo University, Giza, Egypt*

Abstract

Phenol is an extremely hazardous and toxic aromatic compound. Its presence in wastewater endangers human health and the environment as well. The present work employs a novel carrier/catalyst system for heterogeneous Fenton's oxidation of phenol in wastewaters. $CuFe_2O_4$ (CuF) was synthesized via a modified sol-gel technique to be the catalyst for Fenton's heterogeneous process. The structural aspects of CuF were investigated using XRD and TEM. CuF was then loaded into NBR carrier employing an open mill rubber processing machine. Oxidation of phenol in synthetic wastewater was carried out in a standard 1L continuous stirred tank reactor. Different operating conditions viz. time, pH, and oxidant concentration, were optimized using Box-Behnken design. H_2O_2/catalyst (w/w) ratio was varied in the range from 10-20, contact time from 60-90 min and pH from 3 to 5, while initial phenol concentration in aqueous solution was fixed at the level of 300 ppm. Response surface methodology (RSM) plot showed that phenol removal reached 85.4 % as a maximum value at the optimum operating parameters of 4.208, 14.35, and 69.568 for pH, H_2O_2/catalyst, and contact time respectively.

Keywords: Fenton; phenol; wastewater, ferrite; rubber; Box-Behnken

1. Introduction

Phenolic compounds, in wastewaters, is a verified source of risk and hazards to the environment as well as human beings [1. Phenol is a very well-known potent toxicant which can enhance free radical generation and thus might end to carcinogenesis or other severe health-related problems [2].

Phenolic compounds are commonly discharged from many chemical industrial processes such as insecticides, pesticides, pharmaceuticals, and petroleum refineries [3]. Phenols are byproducts of aromatic hydrocarbon oxidation pathways and from acidic oil extraction processes [3]. Phenolic wastewaters is also a commonly produced from oil milling agro-industries e.g. olive oil mills [4].

The natural secondary biological degradation of phenolic wastewaters is considered extremely difficult [5]. This is directly related to the inactivation of natural bacterial growth by phenol [6] as well as its intermediates like hydroquinone, benzoquinone, catechol, resorcinol, maleic acid, oxalic acid, salicylic acid, 1,2,3- benzotriol, and muconic acid [7]. Thus advanced oxidation processes (AOP) have been developed for the degradation of phenols in wastewater [8]. AOP's depend on the ability of $OH^\bullet$ free radicals to attacks the aromatic phenolic ring [8].

Fenton's process is the most promising AOP due to its ability to almost completely mineralize phenols [9]. Classical homogeneous Fenton's process depends on a preliminary dissociation of H_2O_2 by Fe^{2+} [10]:

$$Fe^{2+} + H_2O_2 \rightarrow OH^- + OH^\bullet + Fe^{3+}$$

However, the homogeneous Fenton's process suffers from several crippling drawbacks including: narrow pH range, secondary iron sludge generation, and difficult Fe^{+2}/Fe^{+3} recycling [11]. Using a heterogeneous catalyst served well in this area. However, the choice of a suitable catalyst and the optimization process parameter remain cumbersome.

Ferrites have long been used as heterogeneous Fenton's catalysts [10]. They offer great flexibility regarding the ease of application as well as their easy

*Corresponding author e-mail: salem-gaballah@cu.edu.eg; (S.M. Salem-Gaballah)
Receive Date: 08 August 2023, Revise Date: 01 October 2023, Accept Date: 09 October 2023
DOI: https://doi.org/10.21608/ejchem.2023.227999.8395

magnetic separation. Copper ferrite ($CuFe_2O_4$) is one of the most successful ferrite catalysts. It has been successfully applied for degradation of phenol [12], p-nitrophenol and p-aminophenol [13], and gallic acid [14]. $CuFe_2O_4$ can be generally regarded as a bimetallic catalyst. The synergistic combination of Fe^2, Cu^{2+} achieves better H_2O_2 decomposition [15]. In addition to Fe^2, Cu^{2+} also enhances H_2O_2 decomposition [12]:

$Cu^{2+} + H_2O_2 \rightarrow Cu^+ + H^+ + HO_2^{\bullet}$

Moreover, Cu^+ facilitates Fe^{+3} recycling to Fe^{2+} [15]:

$Fe^{3+} + Cu^+ \rightarrow Fe^{2+} + Cu^{2+}$

Loading $CuFe_2O_4$ (CuF) into an inert rubbery carrier such as nitrile butadiene rubber (NBR), facilitates the degradation of phenol. The inert carrier enhances phenol adsorption and thus achieves better contact [16] and accordingly fasten phenol degradation. On the other hand, CuF/NBR beads are easy to separate from the mother liquor to be reuse again. This approach has not been covered before in any research paper.

The current research aims at exploring the oxidative capabilities of the novel CuF/NBR nanocomposites for degradation of phenol in aqueous solution, and optimizing various process parameters e.g. H_2O_2, contact time and pH, which can affect Fenton's oxidation process.

Materials and methods

Chemical synthesis of CuFe₂O₄

$CuFe_2O_4$ spinel ferrite nanoparticles have been synthesized using Citrate-nitrate sol-gel method [17] according to the following equation:

$2\ Fe(NO_3)_3 + Cu(NO_3)_2 \rightarrow CuFe_2O_4 + 8\ NO_2 + 4\ O_2$

The initial solution contains stoichiometric proportions of $Fe(NO_3)_3.9H_2O$ and $Cu(NO_3)_2$ (Alpha Chemicals), together with citric acid. The solution was preheated to 65ºC. Aqueous ammonia (33% w/v) solution was then added drop by drop under constant stirring till pH becomes neutral. The solution was allowed to evaporate to obtain the gel phase. Self-ignition takes place to form a fluffy loose powder which was then sintered at 500ºC for 5 hours in a muffle furnace.

Material characterization

X-ray diffraction analysis was carried out using a Proker D_8 advance X-ray diffractometer with Cu K_α radiation (λ = 1.5418 Å). Morphology of $CuFe_2O_4$ nanoparticles was investigated using Transmission Electron Microscope (TEM) (JEOL-1010). On the other hand, Vibrating sample magnetometer (VSM) (Lake Shore, Model-7410) was used to study magnetic properties and to obtain magnetic hysteresis loops.

Preparation of CuF/NBR beads

Nitrile butadiene rubber (NBR) was supplied by the transport and engineering company (Alexandria, Egypt). CuF/NBR nanocomposites were prepared according to ASTM D3182-07 [18], in a two roll-mixing mill with outside diameter 470 mm, working distance 300 mm, rolling speed 24 rpm and fraction ratio of (1 : 1.4)

100 g of NBR, and 2 g stearic acid were blended with CuF with the aid of 50 g dioctyl phthalate plasticizer and 5g ZnO (NBR activator) in an open mill mixer. 2 g sulfur were then added for crosslinking of rubbery matrix. The vulcanization was carried out by pressing at 155±2 °C and 4 MPa (150 bar) for 30 minutes.

Fenton's heterogeneous oxidation

Heterogeneous Fenton's oxidation experiments were carried out in a 1.0 L stainless-steel continuous stirred-tank reactor (CSTR) [19]. Phenol crystals (98% purity, Alpha Chemicals) have been used to prepare synthetic wastewater solution at a concentration level of 300 mg/L. CuF/NBR beads were then added to wastewater followed by the addition of H_2O_2 to initiate Fenton's oxidation. The reaction was stopped at the specified intervals by adding NaOH solution [20]. The supernatant was then separated and heated to 50°C under shaking to expel any remaining H_2O_2. And finally, the solution was then filtered and settled before being chemically analysed for the remaining phenol concentration.

Analysis of phenol concentration

Determination of phenol was performed according to ASTM D1783-01 [21]. Phenol was allowed to complex with 4-aminoantipyrine at pH 10 in the presence of potassium hexacyanoferrate (III). A reddish adduct was obtained with λ_{max} of 460 nm. Absorption was measured using a computerized spectrophotometer (Shimadzu). Phenol removal percentage was calculated from:

$$\text{Phenol removal } \% = \frac{A_o - A_t}{A_o} \times 100$$

where A_o is the initial absorbance and A_t is the absorbance at time t .

Experimental design

There are three variable process parameters namely pH, H_2O_2 /catalyst, and contact time, which are well known to affect Fenton's process. The interaction among these process parameters, nominated here as A, B, and C, was studied using Box-Behnken factorial design [22] employing three levels. The latter have been determined following preliminary pilot experiments for each parameter separately. Optimization was achieved through response surface methodology (RSM) [19], with the aid of Design-Expert software (v.10) [22]. The relation between independent variables are fitted to a second order model according to [23]:

$$Y = \beta_0 + \sum_{i=1}^{k} \beta_i x_i + \sum_{i=1}^{k} \beta_{ii} x_i^2 + \sum_{i=1}^{k-1} \sum_{j=2}^{k} \beta_{ij} x_i x_j + \varepsilon$$

where Y is the response; β_0 is a constant coefficient; β_i , β_{ii}, and β_{ij} are the coefficients for the linear, quadratic, and interaction effects, respectively; x_i and x_j are the coded levels for the independent variables i.e. A, B, or C; k is the number of independent variables; and ε is the random error.

Results and Discussion

X-ray diffraction analysis of $CuFe_2O_4$

Figure (1) shows X-ray diffraction pattern of $CuFe_2O_4$ as compared with ICDD card [00-034-0425]. A single phase $CuFe_2O_4$ sample was obtained in a spinel structure with space group (I41/amd). The interplanar spacing (d) values and peak relative intensities are in good agreement with those reported in ICDD card [00-034-0425] of $CuFe_2O_4$. Crystallite size of $CuFe_2O_4$ was calculated using Scherrer's formula [24] and found to be 39 nm.

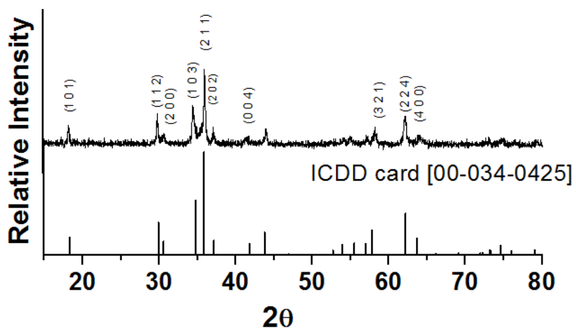

Fig. (1): X-ray diffractogram of $CuFe_2O_4$ as compared with ICDD [00-034-0425] .

TEM imaging of $CuFe_2O_4$ nanoparticles

High resolution transmission electron microscopic (HRTEM) images for the synthesized $CuFe_2O_4$ sample is presented in Figure (2).

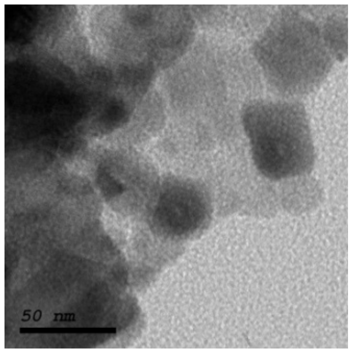

Fig. (2): TEM image of *$CuFe_2O_4$* nanoparticles

TEM image shows cuboidal morphology for $CuFe_2O_4$ with length of 38 nm and width of 39 nm.

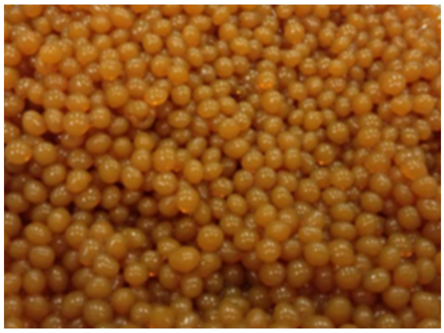

Fig. (3): Optical photograph of CuF/NBR beads.

Figure (3) shows an optical photograph of the obtained CuF/NBR beads. They appear similar with a nearly spherical shape and diameter range 500-700 μm.

Figure (4) shows a plot of the variation of magnetization (M) with magnetic field (H). Both $CuFe_2O_4$ and CuF/NBR beads show the usual M-H hysteresis loop characteristic of a soft ferromagnetic system [24] with very low coercive magnetic field.

Table (1): Experimental and predicted responses [phenol removal (%)] for different experimental runs

Run	Coded factors			Factor experimental values			Response values (Phenol removal %)	
	A	B	C	pH	H_2O_2/ catalyst (w/w)	Contact Time (min)	Experi m- ental	predicted
1	−1	−1	0	3	10	75	72.01	71
2	1	−1	0	5	10	75	72.7	72.635
3	−1	1	0	3	20	75	72.77	72.835
4	1	1	0	5	20	75	70.46	71.0525
5	−1	0	−1	3	15	60	75.83	76.3438
6	1	0	−1	5	15	60	73.04	73.0263
7	−1	0	1	3	15	90	74.82	74.8338
8	1	0	1	5	15	90	78.1	77.5863
9	0	−1	−1	4	10	60	76.53	76.6088
10	0	1	−1	4	20	60	68.57	67.9913
11	0	−1	1	4	10	90	69.02	69.5988
12	0	1	1	4	20	90	78.13	78.0513
13	0	0	0	4	15	75	85.75	85.77
14	0	0	0	4	15	75	85.75	85.77
15	0	0	0	4	15	75	85.75	85.77

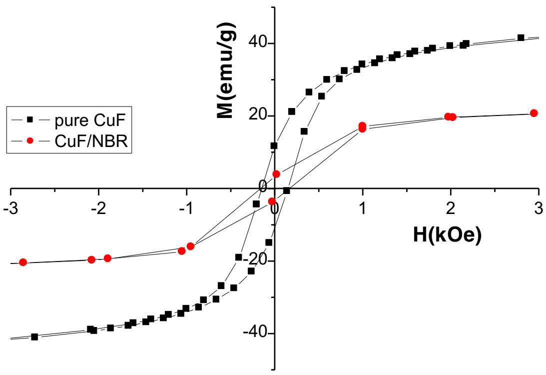

Fig. (4): M-H plot for CuF and CuF/NBR beads.

The lack of reversibility in M(H) relation is the origin of magnetic hysteresis. The magnetic behaviour as well as the calculated properties of CuF/NBR is generally less than pure $CuFe_2O_4$ due to the dilution of the latter by the inert rubbery matrix. For example, remnant magnetizations i.e. M at zero magnetic field, were found to be 11.85 and 5.98 emu/g for $CuFe_2O_4$ and CuF/NBR beads respectively.

The small hysteresis loop of CuF/NBR beads indicate low degree of irreversibility of M-H hysteresis. On the other hand, the soft ferromagnetic character of CuF/NBR beads was deduced from the rather small squareness ratio (M_r/M_s) which was found to be 0.14328. This makes these beads very suitable for magnetic separation systems and for recyclability.

Box-Behnken design factorial design for the three process variables is shown in table (1) at three experimental levels for each. Their allowed values include {-1,0,1} for the low, mid, and high levels respectively.

Fifteen experimental runs are needed for this experimental design which were generated with the aid of Design-Expert (v 10) software. The last three runs in table (1) are important to test for the validity of the model. They have been carried out at the three mid values of the interacting parameters i.e. at 4, 15, and 75 minutes for pH, H_2O_2/catalyst, and contact time respectively.

Response values in table (1) represent phenol removal percentage obtained for each of the fifteen runs. These responses were fed as input data into Design-Expert (v 10) software and the following second order polynomial equation has been obtained:

$$Phenol\ removal\ \% = 85.77 - 0.14125\,A - 0.04125B + 0.7625C - 0.75AB + 1.5175AC + 4.2675\,BC - 5.7A^2 - 8.085B^2 - 4.6225C^2$$

where A,B, and C are the coded process variables for pH, H_2O_2/catalyst, and contact time respectively .

The value for maximum phenol removal efficiency was predicted by Design-Expert (v 10) software to around 85.75 % as shown in figure (5). There is great congruency between the predicted maximum value and the practically found response from the experimental run at an average of 85.4 %.

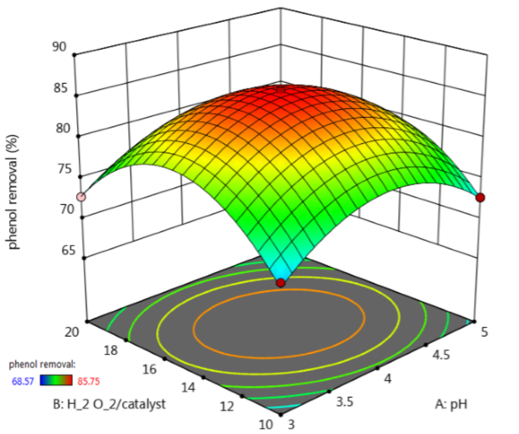

Fig. (5): 3D diagram of the second degree polynomial surface showing maximum phenol removal of 85.75%.

The optimum values for the three parameters were calculated from the polynomial equation and found to be 4.208, 14.35, and 69.568 for pH, H_2O_2/catalyst, and contact time respectively.

A good congruence between the experimental and predicted response values proves the validity of the model and the presence of the optimal point as shown in figure (6).

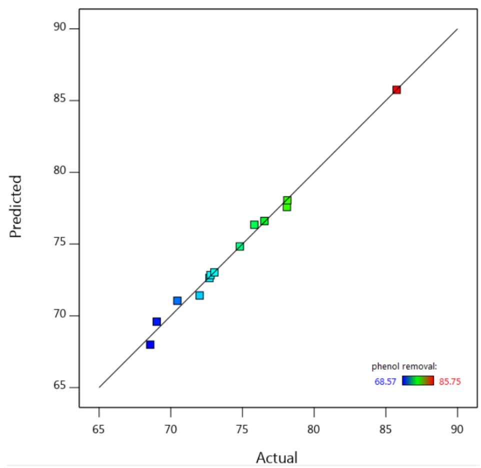

Fig. (6): Values of the predicted versus experimental responses

Table (2): p-values corresponding to different coefficients

	A	B	C	AB	AC	BC	A^2	B^2	C^2
coefficient	-0.14125	-0.04125	0.7625	-0.75	1.5175	4.2675	-5.7	-8.085	-4.6225
p-values	0.5478	0.8581	0.0177	0.0601	**0.0045**	**<0.0001**	**<0.0001**	**<0.0001**	**<0.0001**

The high correlation coefficient (R^2=0.9925) indicated that the model predicted by Design-Expert (v 10) software was suitable enough for calculating phenol removal as a function of pH, H_2O_2/catalyst, and contact time.

In addition, NOVA analysis has been applied to define the significance of each parameter. The p values, *for* each of the three factors are presented in table (2). Those interaction factors with p-values ≤ 0.05 are the only significant. This condition is valid only for A^2, B^2, C^2, AC, and BC, which represent the interacting factors.

It was noticed that catalyst/carrier system was durable enough and could be magnetically separated to be reused for three successive Fenton's processes with loss of efficiency < 7% after the third run.

4. Conclusions

In this study, $CuFe_2O_4$/NBR beads have been used as catalyst/carrier system for Fenton's heterogeneous oxidation applied for the degradation of phenolic synthetic wastewater. $CuFe_2O_4$ was first synthesized by a modified sol-gel technique and then incorporated in NBR matrix using open mill rubber homogenizer. The effect of the three interacting process parameters viz. pH, H_2O_2/catalyst, and contact time on phenol oxidation rate was studied following Box-Behnken factorial design. RSM optimization led to a maximum phenol removal of 85.75% at optimum operating conditions of 4.208, 14.35, and 69.568 for pH,

H_2O_2/catalyst, and contact time respectively. The obtained results suggest that $CuFe_2O_4$/NBR beads could be efficiently used as carrier/catalyst system in Fenton's oxidation process including Fenton's fluidized bed reactor (FBR).

Conflicts of interest

"There are no conflicts to declare".

References

[1] Sun, J., Mu, Q., Kimura, H., Murugadoss, V., He, M., Du, W., & Hou, C. (2022). Oxidative degradation of phenols and substituted phenols in the water and atmosphere: a review. *Advanced Composites and Hybrid Materials*, *5*(2), 627-640.

[2] Ismail, M., Akhtar, K., Khan, M. I., Kamal, T., Khan, M. A., M Asiri, A., Seo, J. & Khan, S. B. (2019). Pollution, toxicity and carcinogenicity of organic dyes and their catalytic bio-remediation. *Current pharmaceutical design*, *25*(34), 3645-3663.

[3] Jabbar, Z. H., & Graimed, B. H. (2022). Recent developments in industrial organic degradation via semiconductor heterojunctions and the parameters affecting the photocatalytic process: A review study. *Journal of Water Process Engineering*, *47*, 102671.

[4] Andiloro, S., Bombino, G., Denisi, P., Folino, A., Zema, D. A., & Zimbone, S. M. (2021). Depuration performance of aerated tanks simulating lagoons to treat olive oil mill wastewater under different airflow rates, and concentrations of polyphenols and nitrogen. *Environments*, *8*(8), 70.

[5] Krastanov, A., Alexieva, Z., & Yemendzhiev, H. (2013). Microbial degradation of phenol and phenolic derivatives. *Engineering in Life Sciences*, *13*(1), 76-87.

[6] Kauffmann, A. C., & Castro, V. S. (2023). Phenolic Compounds in Bacterial Inactivation: A Perspective from Brazil. *Antibiotics*, *12*(4), 645.

[7] Gan, W., Ge, Y., Zhong, Y., & Yang, X. (2020). The reactions of chlorine dioxide with inorganic and organic compounds in water treatment: kinetics and mechanisms. *Environmental Science: Water Research & Technology*, *6*(9), 2287-2312.

[8] Kroflič, A., Schaefer, T., Huš, M., Le, H. P., Otto, T., & Herrmann, H. (2020). OH radicals reactivity towards phenol-related pollutants in water: temperature dependence of the rate constants and novel insights into the [OH–phenol]˙ adduct formation. *Physical Chemistry Chemical Physics*, *22*(3), 1324-1332.

[9] Brillas, E., & Garcia-Segura, S. (2020). Benchmarking recent advances and innovative technology approaches of Fenton, photo-Fenton, electro-Fenton, and related processes: A review on the relevance of phenol as model molecule. *Separation and Purification Technology*, *237*, 116337.

[10] Thomas, N., Dionysiou, D. D., & Pillai, S. C. (2021). Heterogeneous Fenton catalysts: A review of recent advances. *Journal of Hazardous Materials*, *404*, 124082.

[11] Watwe, V. S., Kulkarni, S. D., & Kulkarni, P. S. (2021). Cr (VI)-mediated homogeneous Fenton oxidation for decolorization of methylene blue dye: Sludge free and pertinent to a wide pH range. *ACS omega*, *6*(41), 27288-27296.

[12] Hamdan, N., Haija, M. A., Banat, F., & Eskhan, A. (2017). Heterogeneous catalytic degradation of phenol by a Fenton-type reaction using copper ferrites ($CuFe_2O_4$). *Desalination and Water Treatment*, *69*, 268-283.

[13] Moreno-Castilla, C., López-Ramón, M. V., Fontecha-Cámara, M. Á., Álvarez, M. A., & Mateus, L. (2019). Removal of phenolic compounds from water using copper ferrite nanosphere composites as fenton catalysts. *Nanomaterials*, *9*(6), 901.

[14] López-Ramón, M. V., Álvarez, M. A., Moreno-Castilla, C., Fontecha-Cámara, M. A., Yebra-Rodríguez, Á., & Bailón-García, E. (2018). Effect of calcination temperature of a copper ferrite synthesized by a sol-gel method on its structural characteristics and performance as Fenton catalyst to remove gallic acid from water. *Journal of colloid and interface science*, *511*, 193-202.

[15] Bosio, G. N., García Einschlag, F. S., Carlos, L., & Mártire, D. O. (2023). Recent Advances in the Development of Novel Iron–Copper Bimetallic Photo Fenton Catalysts. *Catalysts*, *13*(1), 159.

[16] Chen, Z., Oh, W. D., & Yap, P. S. (2022). Recent advances in the utilization of immobilized laccase for the degradation of phenolic compounds in aqueous solutions: A review. *Chemosphere*, 135824.

[17] Ali, T. M., Ismail, S. M., Mansour, S. F., Abdo, M. A., & Yehia, M. (2021). Physical properties of Al-doped cobalt nanoferrite prepared by citrate–nitrate auto combustion method. *Journal of Materials Science: Materials in Electronics*, *32*(3), 3092-3103.

[18] Khattak, A., & Amin, M. (2016). Accelerated aging investigation of high voltage EPDM/silica composite insulators. *Journal of Polymer Engineering*, *36*(2), 199-209.

[19] Zaher, A. (2020). Photo-Catalytic degradation of phenol wastewater: optimization using response surface methodology. *Egyptian Journal of Chemistry*, *63*(11), 4439-4445.

[20] Zhu, X., Tian, J., Liu, R., & Chen, L. (2011). Optimization of Fenton and electro-Fenton oxidation of biologically treated coking wastewater using response surface methodology. *Separation and Purification Technology*, *81*(3), 444-450.

[21] Ratnawati, R., Enjarlis, E., Husnil, Y. A., Christwardana, M., & Slamet, S. (2020). Degradation of phenol in pharmaceutical wastewater using TiO_2/pumice and O_3/active carbon.

[22] El Shahawy, A., Mohamadien, R. H., El-Fawal, E. M., Moustafa, Y. M., & Dawood, M. M. K. (2021). Hybrid Photo-Fenton oxidation and biosorption for petroleum wastewater treatment and optimization using Box–Behnken Design. *Environmental Technology & Innovation*, *24*, 101834.

[23] Brillas, E., & Garcia-Segura, S. (2016). Solar Photoelectro-Fenton degradation of acid Orange 7 azo dye in a solar flow plant: optimization by response surface methodology. *Water Conservation Science and Engineering*, *1*, 83-94.

[24] Phuruangrat, A., Kuntalue, B., Thongtem, S., & Thongtem, T. (2016). Synthesis of cubic $CuFe_2O_4$ nanoparticles by microwave-hydrothermal method and their magnetic properties. *Materials Letters*, *167*, 65-68.